

This discussion paper is/has been under review for the journal Biogeosciences (BG).
Please refer to the corresponding final paper in BG if available.

Kinetic bottlenecks to chemical exchange rates for deep-sea animals – Part 1: Oxygen

A. F. Hofmann^{1,*}, E. T. Peltzer¹, and P. G. Brewer¹

¹Monterey Bay Aquarium Research Institute (MBARI), 7700 Sandholdt Road, Moss Landing, CA 95039–9644, USA

*now at: German Aerospace Center (DLR), Institute of Technical Thermodynamics, Pfaffenwaldring 38–40, 70569 Stuttgart, Germany

Received: 9 September 2012 – Accepted: 3 October 2012 – Published: 11 October 2012

Correspondence to: A. F. Hofmann (ahofmann.mbari@gmail.com)

Published by Copernicus Publications on behalf of the European Geosciences Union.

13817

Abstract

Ocean warming will reduce dissolved oxygen concentrations which can pose challenges to marine life. Oxygen limits are traditionally reported simply as a static concentration thresholds with no temperature, pressure or flow rate dependency. Here we
5 treat the oceanic oxygen supply potential for heterotrophic consumption as a dynamic molecular exchange problem analogous to familiar gas exchange processes at the sea surface. A combination of the purely physico-chemical oceanic properties temperature, hydrostatic pressure, and oxygen concentration defines the ability of the ocean to supply oxygen to any given animal. This general oceanic oxygen supply potential is
10 modulated by animal specific properties such as the diffusive boundary layer thickness to define and limit maximal oxygen supply rates. Here we combine all these properties into formal, mechanistic equations defining novel oceanic properties that subsume various relevant classical oceanographic parameters to better visualize, map, comprehend, and predict the impact of ocean deoxygenation on aerobic life. By explicitly
15 including temperature and hydrostatic pressure into our quantities, various ocean regions ranging from the cold deep-sea to warm, coastal seas can be compared. We define purely physico-chemical quantities to describe the oceanic oxygen supply potential, but also quantities that contain organism-specific properties which in a most generalized way describe general concepts and dependencies. We apply these novel
20 quantities to example oceanic profiles around the world and find that temperature and pressure dependencies of diffusion and partial pressure create zones of greatest physical constriction on oxygen supply typically at around 1000 m depth, which coincides with oxygen concentration minimum zones. In these zones, which comprise the bulk of the world ocean, ocean warming and deoxygenation have a clear negative effect
25 for aerobic life. In some shallow and warm waters the enhanced diffusion and higher partial pressure due to higher temperatures might slightly overcompensate for oxygen concentration decreases due to decreases in solubility.

13818

layer driven by partial pressure differences takes place; and, as in knowledge of gas exchange rates at the sea surface (e.g. Wanninkhof, 1992) where wind speed is a critical variable, bulk fluid flow velocity is important. A simple concentration value alone cannot adequately describe this process. For example, giving a concentration as a limit provides no temperature dependent information, so that the same value is assumed to be limiting over a temperature span of possibly 30 °C. This can be overcome to some extent by providing pO_2 as a limiting value (Hofmann et al., 2011), but the rate problem for gas transfer across a diffusive boundary layer contains also terms for diffusivity, and the relationship between boundary layer thickness and velocity over the surface, and thus a much more complete description is required.

Oxygen transport across the respiratory surface diffusive boundary layer is such a critical property that animals typically work to control flow and thus manage the supply of their respiratory rate needs. However there clearly are cases where the physically driven external flow field is controlling (Patterson and Sebens, 1989; Shashar et al., 1993) and is reflected in the physical distribution of organisms. And if O_2 transport is insufficient then either physical work to increase flow and thin the boundary layer is required, or organisms must resort to a temporary draw down of their finite store of alternative internal chemical energy supply.

The challenge here is in providing a useful function that more accurately describes the oceanic supply potential so as to separate as best as possible the purely physical terms which are universally applicable such as temperature T , oxygen concentration $[O_2]$, hydrostatic pressure P (together resulting in an oxygen partial pressure pO_2), diffusivity, and the basic fluid dynamical form of the dependence of boundary thickness on flow, from those properties that are unique to any one animal such as the size of the respiratory surface area and any unique characteristics of basic shape or mode of swimming or pumping.

There is no debate over combining the T , $[O_2]$, P , and diffusivity terms since these are fundamental properties. The difficulty is in providing a better way of including the flow term as a general principle. There is no doubt of the existence of a diffusive

13821

boundary layer that is present at all ocean surfaces, and formal descriptions of this are essential for air-sea gas exchange rates, mineral dissolution rates, and phytoplankton nutrient uptake rates. And in cases where the dimensions of the organism exceed about 1 mm (e.g. Zeebe and Wolf-Gladrow, 2001) the relationship between flow rate and boundary layer thickness is found to be strongly non-linear. The most widely used formulation is based on the dimensionless Schmidt number (e.g. Santschi et al., 1991; Wanninkhof, 1992) and this relationship is standard within the ocean sciences. There are other concepts of larger scale attached water volumes to swimming marine animals (Katija and Dabiri, 2009); these affect the bulk fluid flow properties and thus indirectly boundary layer thickness.

As the base case we use a planar surface model for the molecular exchange surface; although considerable fine structure exists the same basic diffusion rates hold. And while the animal will maintain a boundary layer typical for its respiratory needs, the physical forcing required to change the thickness of this layer will follow the same physical laws. We derive all gas flux properties on a per square centimeter scale so as to provide a way to normalize for different respiratory surface areas.

We stress that the end result of our work here cannot be profiles and maps that better describe O_2 rate limits for all organisms since individual requirements vary enormously. Rather it is the provision of relative profiles and maps that in very much the same way that profiles and maps of simple O_2 concentration values are used today can illuminate which regions of the ocean are better able to support aerobic marine life. And to do so in a more quantitative manner that permits incorporation of changes associated with ocean warming and differentiation with depth and temperature.

13822

diffusion, with the result that L increases. This translates into a higher p_f with depth, i.e. a higher necessary pO_2 to sustain the given oxygen consumption rate E . The limit oxygen concentration C_f initially follows suit, but as hydrostatic pressure increases with depth, so does the pO_2 for a given $[O_2]$ (Enns et al., 1965). This means that p_f , the pO_2 necessary to sustain E , which is more or less constant with depth from below 2000 m, as temperature does not change anymore, is sustained by a smaller and smaller oxygen concentration: C_f decreases from about 2000 m on.

Different ocean basins exhibit markedly different temperature and salinity profiles; these differences affect the quantity C_f since this subsumes the influences of temperature, salinity and hydrostatic pressure on diffusive gas transport. Figure 6 and the fourth column in Table 2 show C_f depth profiles for our example hydrographical stations, assuming a constant current velocity of 2 cm s^{-1} . In the Pacific, the profiles are rather similar, while warm enclosed seas like the Mediterranean differ markedly. Here, due to warm temperatures throughout the water column, the entire profiles are shifted towards lower C_f values. It is remarkable that in the Mediterranean, the oxygen concentration at 4000 m depth required to sustain a given oxygen consumption rate is lower than at the surface. In the Atlantic the C_f maximum is sharply defined at around 1000 m depth; in the Pacific the maximum is more broadly defined at around the same depth, in keeping with classical hydrographic profiles. In the Indian Ocean (Bay of Bengal), the C_f maximum is deeper at ≈ 2000 m. Given the marked similarity of C_f profiles in the Pacific (left panel of Fig. 6), one can conclude that the differences in oxygen supply potential SP_{O_2} between various stations in the Pacific (left panel of Fig. 2) are mainly due to differences in oxygen concentration profiles. This is not the case for the example stations that are not located in the Pacific (right panels of Figs. 2 and 6), where the effects of temperature and pressure considerably contribute to the differences in SP_{O_2} profiles.

Even though our exact description of the dependency is generalized, the fact that the limit oxygen concentration C_f is dependent on current velocity makes it necessary that water flow rates be included in the set of variables that are controlled or reported when

13835

comparing different systems or different animal responses (e.g. Stachowitsch et al., 2007; Riedel et al., 2008; Haselmair et al., 2010). This dependency also indicates that sessile benthic animals in high current environments have an advantage in low oxygen conditions over free swimming fish and over zooplankton that are suspended relatively stationary with respect to the water mass surrounding it. It also explains why under the same low oxygen conditions, continental slopes or the flanks of seamounts experiencing comparatively high mixing rates and currents (van Haren and Gostiaux, 2010) can be more hospitable environments for animals than comparatively stagnant waters.

10 **4.4 First-order estimate of the energy required for mitigation of global change scenarios: Δu_{100}**

In order to investigate which of the multiple effects of warming and deoxygenation will be dominant for certain locations in the ocean, we define the quantity Δu_{100} ; this describes the flow offset from the canonical value of 2 cm s^{-1} needed to keep E_{\max} constant under global warming and deoxygenation scenarios. It is essentially the work that must be done to thin the boundary layer so as to restore a required O_2 uptake rate.

For a first order estimate we assume that the oxygen concentration decreases for a given constant temperature offset by only the difference in the oxygen saturation concentration at every location in the profile. We are aware that this will underestimate true ocean changes, as increased T will also result in higher microbial oxygen consumption rates fueled by the large mass of organic carbon stored in ocean organic matter in sediments, seawater, and sinking particles. Figure 7 and the fifth to seventh columns in Table 2 show Δu_{100} values for all our example stations and 1°C , 2°C , and 3°C warming scenarios.

It can be seen that within the oxygen minimum zone, especially off the Southern California (SC) and the Bay of Bengal (BB) locations, a relatively high flow increase would be needed to compensate for the warming and deoxygenation scenario. As the oxygen concentration becomes small, very high flow rates are necessary to adequately

13836

- Hofmann, A. F., Peltzer, E. T., Walz, P. M., and Brewer, P. G.: Hypoxia by degrees: establishing definitions for a changing ocean, *Deep-Sea Res. Pt. I*, 58, 1212–1226, doi:10.1016/j.dsr.2011.09.004, 2011. 13821
- Houde, E. D. and Schekter, R. C.: Oxygen uptake and comparative energetics among eggs and larvae of three subtropical marine fishes, *Mar. Biol.*, 72, 283–293, doi:10.1007/BF00396834, 1983. 13828
- Hughes, G. M.: The dimensions of fish gills in relation to their function, *J. Exp. Biol.*, 45, 177–195, 1966. 13820, 13830
- Jenkins, W. J.: The biogeochemical consequences of changing ventilation in the Japan/East Sea, *Mar. Chem.*, 108, 137–147, doi:10.1016/j.marchem.2007.11.003, 2008. 13831
- Karp-Boss, L., Boss, E., and Jumars, P.: Nutrient fluxes to planktonic osmotrophs in the presence of fluid motion, *Oceanogr. Mar. Biol. Ann. Rev.*, 34, 71–107, 1996. 13820, 13833
- Katija, K. and Dabiri, J. O.: A viscosity-enhanced mechanism for biogenic ocean mixing, *Nature*, 460, 624–626, doi:10.1038/nature08207, 2009. 13822
- Kemp, W. M., Testa, J. M., Conley, D. J., Gilbert, D., and Hagy, J. D.: Temporal responses of coastal hypoxia to nutrient loading and physical controls, *Biogeosciences*, 6, 2985–3008, doi:10.5194/bg-6-2985-2009, 2009. 13819
- Lazier, J. R. N. and Mann, K. H.: Turbulence and diffusive layers around small organisms, *Deep-Sea Res. Pt. I*, 36, 1721–1733, 1989. 13820, 13833
- Levin, L. A., Ekau, W., Gooday, A. J., Jorissen, F., Middelburg, J. J., Naqvi, S. W. A., Neira, C., Rabalais, N. N., and Zhang, J.: Effects of natural and human-induced hypoxia on coastal benthos, *Biogeosciences*, 6, 2063–2098, doi:10.5194/bg-6-2063-2009, 2009. 13819
- Levitus, S., Antonov, J., and Boyer, T. P.: Warming of the world ocean, *Geophys. Res. Lett.*, 32, 1955–2003, 2005. 13831
- Lyman, J. M., Good, S. A., Gouretski, V. V., Ishii, M., Johnson, G. C., Palmer, M. D., Smith, D. M., and Willis, J. K.: Robust warming of the global upper ocean, *Nature*, 465, 334–337, 2010. 13830, 13831
- Maxime, V., Peyraud-Waitzenegger, M., Claireaux, G., and Peyraud, C.: Effects of rapid transfer from sea water to fresh water on respiratory variables, blood acid-base status and O₂ affinity of haemoglobin in Atlantic salmon (*Salmo salar* L.), *J. Comp. Physiol. B*, 160, 31–39, 1990. 13823
- Middelburg, J. J. and Levin, L. A.: Coastal hypoxia and sediment biogeochemistry, *Biogeosciences*, 6, 1273–1293, doi:10.5194/bg-6-1273-2009, 2009. 13819

13841

- Millero, F. J. and Poisson, A.: International one-atmosphere equation of state of seawater, *Deep-Sea Res. Pt. I*, 28, 625–629, 1981. 13823
- Nakanowatari, T., Ohshima, K. I., and Wakatsuchi, M.: Warming and oxygen decrease of intermediate water in the Northwestern North Pacific, originating from the Sea of Okhotsk, 1955–2004, *Geophys. Res. Lett.*, 34, L04602, doi:10.1029/2006GL028243, 2007. 13830
- Naqvi, S. W. A., Bange, H. W., Fariás, L., Monteiro, P. M. S., Scranton, M. I., and Zhang, J.: Marine hypoxia/anoxia as a source of CH₄ and N₂O, *Biogeosciences*, 7, 2159–2190, doi:10.5194/bg-7-2159-2010, 2010. 13819
- Palumbi, S. R., Sandifer, P. A., Allan, J. D., Beck, M. W., Fautin, D. G., Fogarty, M. J., Halpern, B. S., Incze, L. S., Leong, J.-A., Norse, E., Stachowicz, J. J., and Wall, D. H.: Managing for ocean biodiversity to sustain marine ecosystem services, *Front. Ecol. Environ.*, 7, 204–211, doi:10.1890/070135, 2009. 13820
- Patterson, M. R. and Sebens, K. P.: Forced-convection modulates gas-exchange in Cnidarians, *Proc. Natl. Acad. Sci. USA*, 86, 8833–8836, doi:10.1073/pnas.86.22.8833, 1989. 13821
- Pelster, B. and Burggren, W. W.: Disruption of hemoglobin oxygen transport does not impact oxygen-dependent physiological processes in developing embryos of zebra fish (*Danio rerio*), *Circ. Res.*, 79, 358–362, 1996. 13823, 13827
- Peña, M. A., Katsev, S., Oguz, T., and Gilbert, D.: Modeling dissolved oxygen dynamics and hypoxia, *Biogeosciences*, 7, 933–957, doi:10.5194/bg-7-933-2010, 2010. 13819
- Piiper, J.: Respiratory gas exchange at lungs, gills and tissues: mechanisms and adjustments, *J. Exp. Biol.*, 100, 5–22, 1982. 13823, 13827
- Pinczewski, W. V. and Sideman, S.: A model for mass (heat) transfer in turbulent tube flow, Moderate and high Schmidt (Prandtl) numbers, *Chem. Eng. Sci.*, 29, 1969–1976, doi:10.1016/0009-2509(74)85016-5, 1974. 13846
- Pinder, A. W. and Burggren, W. W.: Ventilation and partitioning of oxygen uptake in the frog *rana pipiens*: effects of hypoxia and activity, *J. Exp. Biol.*, 126, 453–468, 1986. 13823
- Pinder, A. W. and Feder, M. E.: Effect of boundary layers on cutaneous gas exchange, *J. Exp. Biol.*, 154, 67–80, 1990. 13823, 13827
- Poertner, H. O. and Knust, R.: Climate change affects marine fishes through the oxygen limitation of thermal tolerance, *Science*, 315, 95–97, doi:10.1126/science.1135471, 2007. 13831
- R Development Core Team: R: A Language and Environment for Statistical Computing, R Foundation for Statistical Computing, Vienna, Austria, available at: <http://www.R-project.org>, 2010. 13830

13842

- Rabalais, N. N., Díaz, R. J., Levin, L. A., Turner, R. E., Gilbert, D., and Zhang, J.: Dynamics and distribution of natural and human-caused hypoxia, *Biogeosciences*, 7, 585–619, doi:10.5194/bg-7-585-2010, 2010. 13819
- Riedel, B., Zuschin, M., Haselmair, A., and Stachowitsch, M.: Oxygen depletion under glass: behavioural responses of benthic macrofauna to induced anoxia in the Northern Adriatic, *J. Exp. Mar. Biol. Ecol.*, 367, 17–27, doi:10.1016/j.jembe.2008.08.007, 2008. 13836
- Santschi, P. H., Anderson, R. F., Fleisher, M. Q., and Bowles, W.: Measurements of diffusive sublayer thicknesses in the ocean by alabaster dissolution, and their implications for the measurements of benthic fluxes, *J. Geophys. Res.*, 96, 10641–10657, doi:10.1029/91JC00488, 1991. 13822, 13823, 13826, 13833, 13846
- Schlitzer, R.: Ocean Data View 4, available at: <http://odv.awi.de>, 2010. 13830
- Seibel, B. A., Chausson, F., Lallier, F. H., Zal, F., and Childress, J. J.: Vampire blood: respiratory physiology of the vampire squid (*Cephalopoda: Vampyromorpha*) in relation to the oxygen minimum layer, *Exp. Biol. Online*, 4, 1–10, doi:10.1007/s00898-999-0001-2, 1999. 13827, 13828
- Shaffer, G., Olsen, S. M., and Pedersen, J. O. P.: Long-term ocean oxygen depletion in response to carbon dioxide emissions from fossil fuels, *Nat. Geosci.*, 2, 105–109, doi:10.1038/NGEO420, 2009. 13819
- Shashar, N., Cohen, Y., and Loya, Y.: Extreme diel fluctuations of oxygen in diffusive boundary-layers surrounding stony corals, *Biol. Bulletin.*, 185, 455–461, 1993. 13821
- Shaw, D. A. and Hanratty, T. J.: Turbulent mass transfer rates to a wall for large Schmidt numbers, *AIChE J.*, 23, 28–37, doi:10.1002/aic.690230106, 1977. 13846
- Soetaert, K., Petzoldt, T., and Meysman, F.: Marelac: tools for aquatic sciences, available at: <http://CRAN.R-project.org/package=marelac>, r package version 2.1, 2010. 13846
- Stachowitsch, M., Riedel, B., Zuschin, M., and Machan, R.: Oxygen depletion and benthic mortalities: the first in situ experimental approach to documenting an elusive phenomenon, *Limnol. Oceanogr.-Methods*, 5, 344–352, 2007. 13836
- Sternberg, R. W.: Friction factors in tidal channels with differing bed roughness, *Mar. Geol.*, 6, 243–260, doi:10.1016/0025-3227(68)90033-9, 1968. 13846
- Stolper, D. A., Revsbech, N. P., and Canfield, D. E.: Aerobic growth at nanomolar oxygen concentrations, *Proc. Natl. Acad. Sci. USA*, 107, 18755–18760, 2010. 13826
- Stramma, L., Johnson, G. C., Sprintall, J., and Mohrholz, V.: Expanding oxygen-minimum zones in the tropical oceans, *Science*, 320, 655–658, 2008. 13830, 13831

13843

- Tallis, H., Lester, S. E., Ruckelshaus, M., Plummer, M., McLeod, K., Guerry, A., Andelman, S., Caldwell, M. R., Conte, M., Copps, S., Fox, D., Fujita, R., Gaines, S. D., Gelfenbaum, G., Gold, B., Kareiva, P., Kim, C., Lee, K., Papenfus, M., Redman, S., Silliman, B., Wainger, L., and White, C.: New metrics for managing and sustaining the ocean's bounty, *Mar. Policy*, 36, 303–306, doi:10.1016/j.marpol.2011.03.013, 2012. 13820
- van Haren, H. and Gostiaux, L.: A deep-ocean Kelvin–Helmholtz billow train, *Geophys. Res. Lett.*, 37, L03605, doi:10.1029/2009GL041890, 2010. 13836
- van Maaren, C. C., Kita, J., and Daniels, H. V.: Temperature tolerance and oxygen consumption rates for juvenile southern flounder *paralichthys lethostigma* acclimated to five different temperatures, UJNR Technical Report No. 28, 135–140, available at: <http://www.lib.noaa.gov/retiresites/japan/aquaculture/proceedings.htm>, 1999. 13829
- Walsh, W. A., Swanson, C., Lee, C.-S., Banno, J. E., and Eda, H.: Oxygen consumption by eggs and larvae of striped mullet, *Mugil cephalus*, in relation to development, salinity and temperature, *J. Fish Biol.*, 35, 347–358, doi:10.1111/j.1095-8649.1989.tb02987.x, 1989. 13828
- Wanninkhof, R.: Relationship between wind-speed and gas-exchange over the ocean, *J. Geophys. Res.-Oceans*, 97, 7373–7382, 1992. 13821, 13822, 13833, 13846
- Weiss, R. F.: Solubility of nitrogen, oxygen and argon in water and seawater, *Deep-Sea Res.*, 17, 721–735, 1970. 13819
- Weiss, R. F.: Carbon dioxide in water and seawater: the solubility of a non-ideal gas, *Mar. Chem.*, 2, 203–215, 1974. 13819
- Wood, P. E. and Petty, C. A.: New model for turbulent mass transfer near a rigid interface, *AIChE J.*, 29, 164–167, doi:10.1002/aic.690290126, 1983. 13846
- Wyrtki, K.: The oxygen minima in relation to ocean circulation, *Deep-Sea Res.*, 9, 11–23, 1962. 13832, 13838
- Yasumasu, I. and Nakano, E.: Respiratory level of sea urchin eggs before and after fertilization, *Biol. Bulletin.*, 125, 182–187, 1963. 13828
- Zeebe, R. E. and Wolf-Gladrow, D.: CO₂ in Seawater: Equilibrium, Kinetics, Isotopes, no. 65 in Elsevier Oceanography Series, Elsevier, first edn., Amsterdam, 2001. 13822, 13823, 13824
- Zhang, J., Gilbert, D., Gooday, A. J., Levin, L., Naqvi, S. W. A., Middelburg, J. J., Scranton, M., Ekau, W., Peña, A., Dewitte, B., Oguz, T., Monteiro, P. M. S., Urban, E., Rabalais, N. N., Ittekkot, V., Kemp, W. M., Ulloa, O., Elmgren, R., Escobar-Briones, E., and Van der Plas, A. K.: Natural and human-induced hypoxia and consequences for coastal

13844

Table 1. Expressing the DBL thickness L as a function of water flow velocity: a generic planar surface description.

The DBL thickness L can be expressed as the fraction of the temperature-dependent molecular diffusion coefficient D for O_2 in cm^2s^{-1} , calculated from temperature and salinity as given in Boudreau (1996, Chapter 4) using the implementation in the R package *marelac* (Soetaert et al., 2010), and the mass transfer coefficient K (Santschi et al., 1991; Boudreau, 1996)

$$L = \frac{D}{K} \quad (15)$$

K can be calculated for O_2 from the water-flow induced shear velocity u' in cms^{-1} and the dimensionless Schmidt number Sc for O_2 (as calculated by linearly interpolating two temperature dependent formulations for $S = 35$ and $S = 0$ in Wanninkhof, 1992, with respect to given salinity)

$$K = au'Sc^{-b} \quad (16)$$

with parameters a and b : Santschi et al. (1991): $a = 0.078$, $b = \frac{2}{3}$; Shaw and Hanratty (1977) (also given in Boudreau, 1996, $a = 0.0889$, $b = 0.704$); Pinczewski and Sideman (1974) as given in Boudreau (1996): $a = 0.0671$, $b = \frac{2}{3}$; Wood and Petty (1983) as given in Boudreau (1996): $a = 0.0967$, $b = \frac{7}{10}$. Due to small differences we use averaged results of all formulations.

u' can be calculated from the ambient current velocity at 100 cm away from the exchange surface u_{100} and the dimensionless drag coefficient c_{100} (Sternberg, 1968; Santschi et al., 1991; Biron et al., 2004)

$$u' = u_{100} \sqrt{c_{100}} \quad (17)$$

c_{100} is calculated from the water flow velocity u_{100} as (Hickey et al., 1986; Santschi et al., 1991)

$$c_{100} = 10^{-3}(2.33 - 0.0526|u_{100}| + 0.000365|u_{100}|^2) \quad (18)$$

Table 2. Continued.

| depth | [O ₂] | SP _{O₂} | E _{max} | C ₁ | Δ <i>U</i> ₁₀₀ 1°C | Δ <i>U</i> ₁₀₀ 2°C | Δ <i>U</i> ₁₀₀ 3°C |
|-----------|-------------------|-----------------------------|------------------|----------------|----------------------------------|----------------------------------|----------------------------------|
| BB | | | | | | | |
| 0 | 222 | 46 | 233 | 13.88 | -0.030 | -0.059 | -0.089 |
| 50 | 169 | 33 | 160 | 16.10 | -0.017 | -0.033 | -0.048 |
| 100 | 80 | 14 | 65 | 20.05 | 0.053 | 0.114 | 0.183 |
| 200 | 58 | 10 | 43 | 22.73 | 0.120 | 0.265 | 0.440 |
| 300 | 40 | 6 | 28 | 24.94 | 0.249 | 0.587 | 1.073 |
| 400 | 45 | 7 | 29 | 27.19 | 0.226 | 0.525 | 0.943 |
| 500 | 60 | 9 | 37 | 29.24 | 0.151 | 0.338 | 0.574 |
| 600 | 78 | 11 | 45 | 30.98 | 0.099 | 0.216 | 0.354 |
| 700 | 96 | 14 | 54 | 32.19 | 0.066 | 0.142 | 0.228 |
| 800 | 120 | 17 | 65 | 33.06 | 0.037 | 0.078 | 0.124 |
| 900 | 135 | 18 | 72 | 33.53 | 0.024 | 0.050 | 0.080 |
| 1000 | 146 | 20 | 78 | 33.62 | 0.016 | 0.033 | 0.053 |
| 1100 | 153 | 21 | 81 | 33.48 | 0.011 | 0.024 | 0.038 |
| 1200 | 166 | 22 | 87 | 33.22 | 0.003 | 0.007 | 0.013 |
| 1300 | 175 | 24 | 92 | 32.87 | -0.002 | -0.003 | -0.003 |
| 1400 | 188 | 25 | 98 | 32.52 | -0.008 | -0.015 | -0.022 |
| 1500 | 199 | 27 | 104 | 32.17 | -0.013 | -0.025 | -0.037 |
| 2000 | 220 | 30 | 113 | 30.90 | -0.019 | -0.038 | -0.057 |
| 3000 | 225 | 30 | 112 | 28.19 | -0.019 | -0.038 | -0.056 |
| 4000 | 230 | 30 | 114 | 24.87 | -0.020 | -0.040 | -0.059 |
| MD | | | | | | | |
| 0 | 204 | 50 | 268 | 9.97 | -0.048 | -0.103 | -0.167 |
| 50 | 165 | 39 | 207 | 10.66 | -0.032 | -0.070 | -0.114 |
| 100 | 40 | 8 | 42 | 13.53 | 0.144 | 0.315 | 0.523 |
| 200 | 14 | 2 | 11 | 19.97 | 1.065 | 4.891 | Inf |
| 300 | 15 | 2 | 11 | 22.79 | 1.094 | 5.237 | Inf |
| 400 | 15 | 2 | 10 | 23.83 | 1.165 | 6.117 | Inf |
| 500 | 16 | 2 | 11 | 24.59 | 1.079 | 5.084 | Inf |
| 600 | 17 | 3 | 11 | 25.35 | 1.030 | 4.592 | Inf |
| 700 | 22 | 3 | 14 | 26.08 | 0.663 | 2.081 | 7.259 |
| 800 | 25 | 4 | 16 | 26.74 | 0.573 | 1.678 | 4.696 |
| 900 | 32 | 5 | 20 | 27.42 | 0.403 | 1.047 | 2.240 |
| 1000 | 40 | 6 | 24 | 28.09 | 0.299 | 0.728 | 1.392 |
| 1100 | 44 | 6 | 26 | 28.65 | 0.267 | 0.637 | 1.183 |
| 1200 | 50 | 7 | 29 | 29.19 | 0.224 | 0.521 | 0.933 |
| 1300 | 55 | 8 | 31 | 29.66 | 0.198 | 0.453 | 0.794 |
| 1400 | 67 | 9 | 37 | 30.16 | 0.146 | 0.324 | 0.547 |
| 1500 | 75 | 10 | 40 | 30.47 | 0.123 | 0.270 | 0.449 |
| 2000 | 106 | 14 | 53 | 32.05 | 0.066 | 0.141 | 0.226 |
| 3000 | NA | NA | NA | NA | NA | NA | NA |
| 4000 | NA | NA | NA | NA | NA | NA | NA |

13849

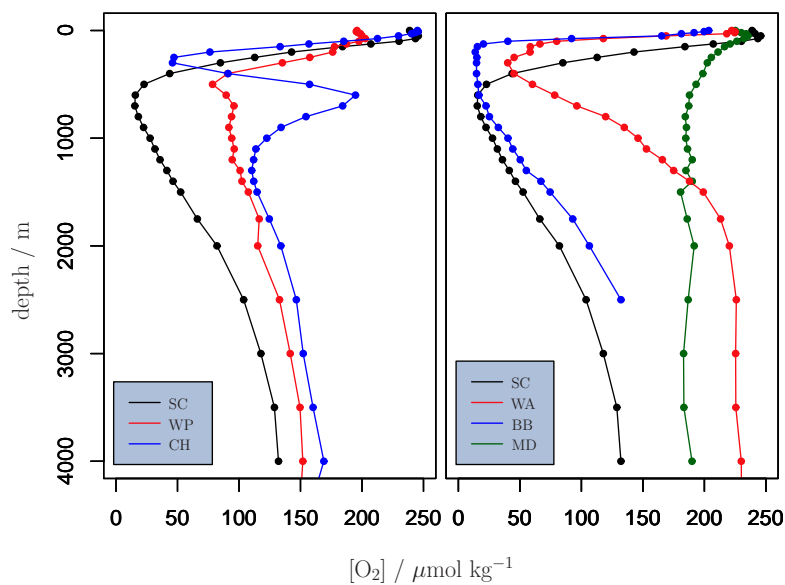


Fig. 1. [O₂] depth profiles of the water column at different hydrographical stations around the world (SC: Southern California (120.5° W, 29.5° N); CH: Chile (75.5° W, 33.5° S); WP: Western Pacific (126.5° E, 11.5° N), WA: Western Africa (6.5° E, 15.5° S), MD: Mediterranean (18.5° E, 35.5° N); BB: Bay of Bengal (87.5° E, 18.5° N)).

13850

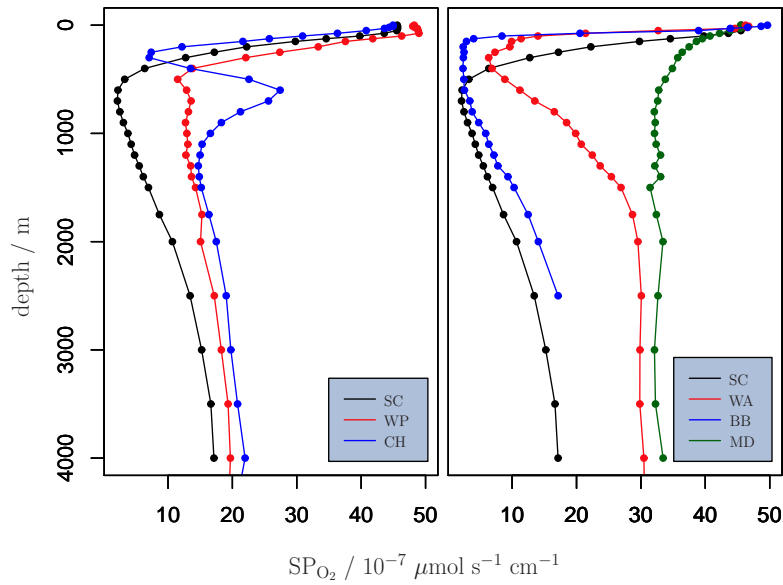


Fig. 2. Oxygen supply potential SP_{O_2} depth profiles of the water column at different hydrographical stations around the world (SC: Southern California (120.5° W, 29.5° N); CH: Chile (75.5° W, 33.5° S); WP: Western Pacific (126.5° E, 11.5° N), WA: Western Africa (6.5° E, 15.5° S), MD: Mediterranean (18.5° E, 35.5° N); BB: Bay of Bengal (87.5° E, 18.5° N)).

13851

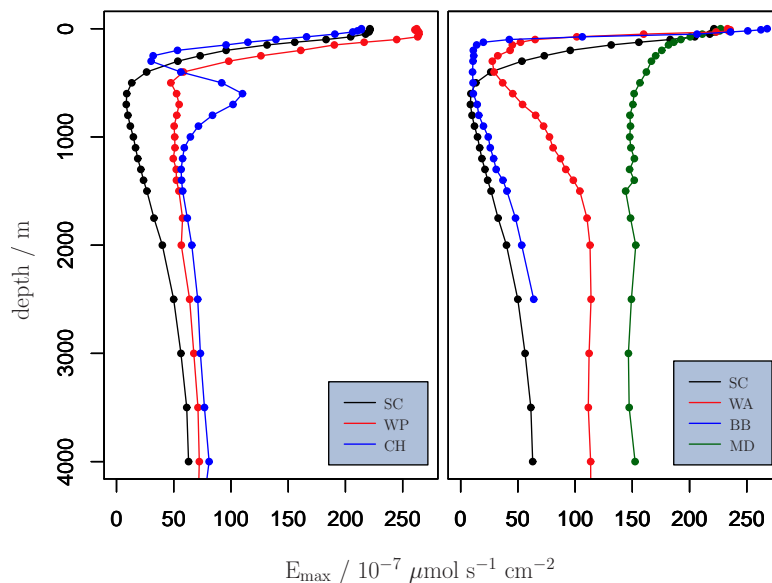


Fig. 3. Generic maximal theoretical oxygen supply rate E_{\max} depth profiles of the water column at different hydrographical stations around the world (SC: Southern California (120.5° W, 29.5° N); CH: Chile (75.5° W, 33.5° S); WP: Western Pacific (126.5° E, 11.5° N), WA: Western Africa (6.5° E, 15.5° S), MD: Mediterranean (18.5° E, 35.5° N); BB: Bay of Bengal (87.5° E, 18.5° N)). A generic flow velocity of $u_{100} = 2 \text{ cm s}^{-1}$ is assumed for all depths to calculate L . If available, detailed flow profiles can be used here, as well as organism-specific descriptions for L .

13852

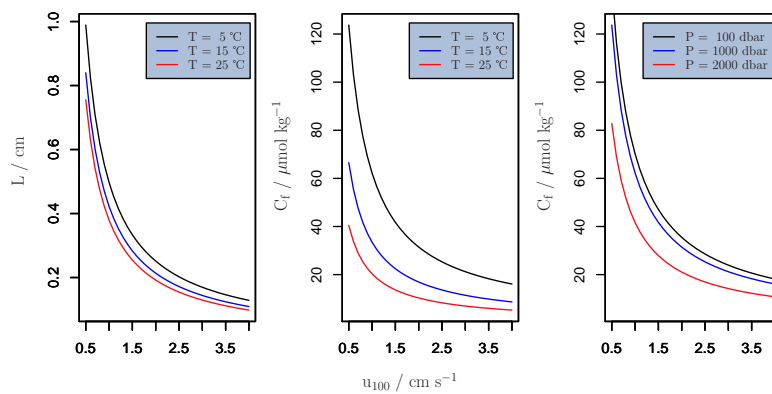


Fig. 4. The influence of flow velocity u_{100} , temperature T and hydrostatic pressure P on the DBL thickness L and C_f , the minimal oxygen concentration supporting a given, laboratory determined oxygen uptake rate E . The dependency of L (and all derived quantities) on u_{100} is based on the simple exemplary model description employed here. While individual organism-specific dependencies may vary in detail, the general dependency of L on the flow velocity is captured here. Unless stated otherwise in the legend: Latitude = 29.5° N, $S = 34$, $T = 5^\circ$ C, $P = 100$ bar, $E = 20 \times 10^{-7} \mu\text{mols}^{-1} \text{cm}^{-2}$, $T_E = 5^\circ$ C, and $S_E = 34$.

13853

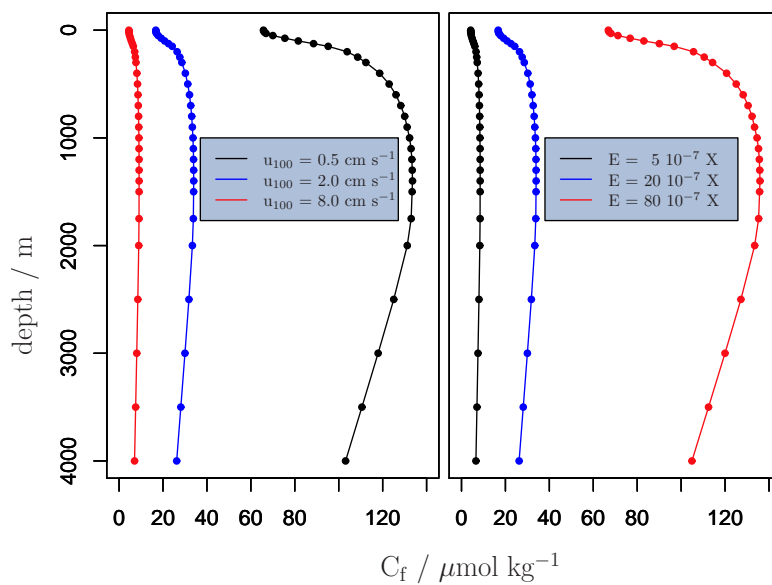


Fig. 5. The influence of flow velocity u_{100} and the given, laboratory-determined oxygen uptake rate E ($X = \mu\text{mols}^{-1} \text{cm}^{-2}$), along depth profiles of temperature T , and hydrostatic pressure P at the Pacific station SC off Southern California (120.5° W, 29.5° N). $T_E = 5^\circ$ C, and $S_E = 34$.

13854

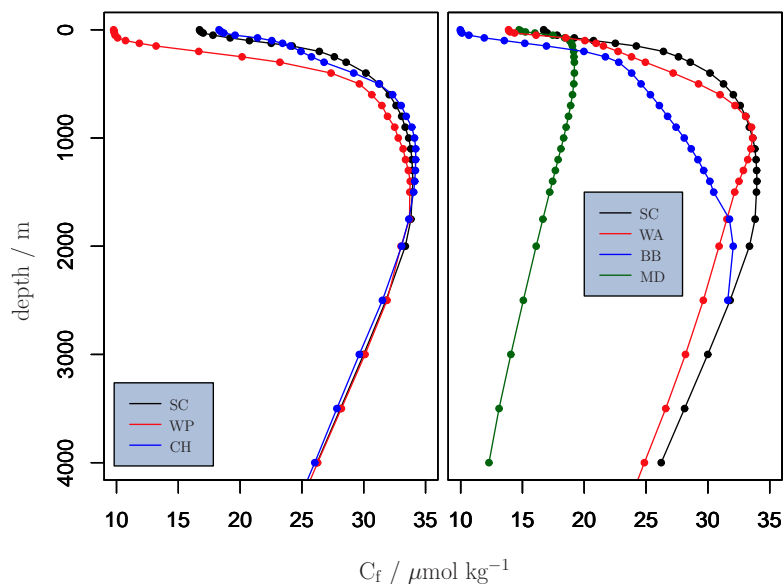


Fig. 6. Minimal oxygen concentration C_t , supporting a given, laboratory determined oxygen uptake rate, depth profiles of the water column at different hydrographical stations around the world (SC: Southern California (120.5° W, 29.5° N); CH: Chile (75.5° W, 33.5° S); WP: Western Pacific (126.5° E, 11.5° N), WA: Western Africa (6.5° E, 15.5° S), MD: Mediterranean (18.5° E, 35.5° N); BB: Bay of Bengal (87.5° E, 18.5° N)). A generic flow velocity of $u_{100} = 2 \text{ cms}^{-1}$ is assumed for all depths to calculate L . If available, detailed flow profiles can be used here, as well as organism-specific descriptions for L .

13855

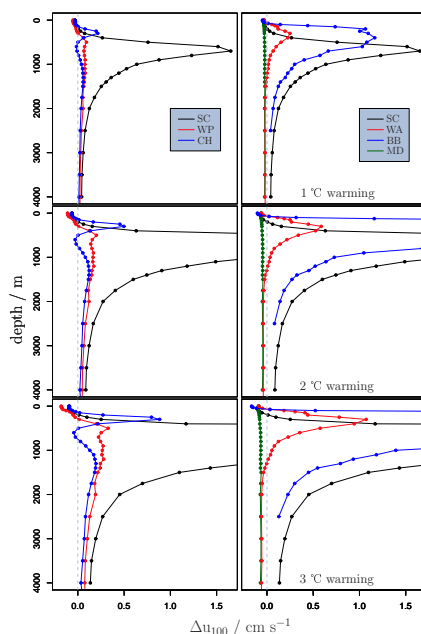


Fig. 7. Flow offset Δu_{100} that would be required to keep E_{max} constant under three ocean warming and deoxygenation scenarios (1°C, 2°C, 3°C) along a set of temperature, salinity and pressure depth profiles of the water column at different hydrographical stations around the world (SC: Southern California (120.5° W, 29.5° N); CH: Chile (75.5° W, 33.5° S); WP: Western Pacific (126.5° E, 11.5° N), WA: Western Africa (6.5° E, 15.5° S), MD: Mediterranean (18.5° E, 35.5° N); BB: Bay of Bengal (87.5° E, 18.5° N)); Assumed generic base flow value: $u_{100}^{\text{base}} = 2 \text{ cms}^{-1}$. At every point $[O_2]$ is assumed to decrease according to the offset in oxygen saturation concentration, using in-situ T as base value and applying the respective assumed temperature change. Positive values of Δu_{100} indicate that the flow would have to be increased from the base value of 2 cms^{-1} to compensate for the combined warming and deoxygenation effects, negative values indicate that a slower flow would suffice to provide the same E_{max} , as in the base case. To not loose details on the small scale and to limit the plots to meaningful values, we truncated the abscissa to Δu_{100} values $\leq 1.65 \text{ cms}^{-1}$.

13856